The relationship between tibiofemoral geometry and musculoskeletal function during normal activity

Published Version:
Martelli S., Sancisi N., Conconi M., Pandy M.G., Kersh M.E., Parenti-Castelli V., et al. (2020). The relationship between tibiofemoral geometry and musculoskeletal function during normal activity. GAIT & POSTURE, 80, 374-382 [10.1016/j.gaitpost.2020.06.022].

Availability:
This version is available at: https://hdl.handle.net/11585/807782 since: 2024-05-09

Published:
DOI: http://doi.org/10.1016/j.gaitpost.2020.06.022

THE RELATIONSHIP BETWEEN TIBIOFEMORAL GEOMETRY AND MUSCULOSKELETAL FUNCTION DURING NORMAL ACTIVITY

Saulo Martelli[1,2], Nicola Sancisi[3], Michele Conconi[3], Marcus G. Pandy[4], Mariana E. Kersh[5], Vincenzo Parenti-Castelli[3], Karen Reynolds[1]

[1] Medical Device Research Institute, College of Science and Engineering, Flinders University, Bedford Park, Australia
[2] North West Academic Centre, University of Melbourne, St Albans, Australia
[3] Department of Industrial Engineering, University of Bologna, Bologna, Italy
[4] Department of Mechanical Engineering, University of Melbourne, Parkville, Australia
[5] Department of Mechanical Science and Engineering, University of Illinois at Urbana-Champaign, USA

ORCID:
Saulo Martelli: orcid.org/0000-0002-0012-8122
Nicola Sancisi: orcid.org/0000-0003-3005-6489
Michele Conconi: orcid.org/0000-0003-2392-2684
Marcus Pandy: orcid.org/0000-0001-9234-1782
Mariana Kersh:
Vincenzo Parenti-Castelli: orcid.org/0000-0001-7328-5957
Karen Reynolds: orcid.org/0000-0002-8273-1610

Original article submission to Gait & Posture.

Introduction to References: 3079 words; Abstract: 298 words

Corresponding author:
Saulo Martelli, Ph.D.
Medical Device Research Institute
College of Science and Engineering
Flinders University
South Rd, Tonsley SA 5042, Australia
E-mail: saulo.martelli@flinders.edu.au

Abstract

Background

The effect of tibiofemoral geometry on musculoskeletal function is important to movement biomechanics.

Research question

We hypothesised that tibiofemoral geometry determines tibiofemoral motion and musculoskeletal function. We then aimed at 1) modelling tibiofemoral motion during normal activity as a function of tibiofemoral geometry in healthy adults; and 2) quantifying the effect of tibiofemoral geometry on musculoskeletal function.

Methods

We used motion data for six activity types and CT images of the knee from 12 healthy adults. Geometrical variation of the tibia and femoral articular surfaces were measured in the CT images. The geometry-based tibiofemoral motion was calculated by fitting a parallel mechanism to geometrical variation in the cohort. Matched musculoskeletal models embedding the geometry-based tibiofemoral joint motion and a common generic tibiofemoral motion of reference were generated and used to calculate joint angles, net joint moments, muscle and joint forces for the six activities analysed. The tibiofemoral model was validated against bi-planar fluoroscopy measurements for walking for all the six planes of motion. The effect of tibiofemoral geometry on musculoskeletal function was the difference between the geometry-based model and the model of reference.

Results

The geometry-based tibiofemoral motion described the pattern and the variation during walking for all six motion components, except the pattern of anterior tibial translation. Tibiofemoral geometry had moderate effect on cohort-averages of musculoskeletal function (R^2 = 0.60 – 1), although its effect was high in specific instances of the model, outputs and activities analysed, reaching 2.94 BW for the ankle reaction force during stair descent. In conclusion, tibiofemoral geometry is a major determinant of tibiofemoral motion during walking.

Significance

Geometrical variations of the tibiofemoral joint are important for studying musculoskeletal function during normal activity in specific individuals but not for studying cohort averages of musculoskeletal function. This finding expands current knowledge of movement biomechanics.

1. Introduction

Joint angles, net moments, and musculoskeletal forces are commonly calculated by assuming a generic model of tibiofemoral motion adapted to each participant in a variety of clinical and research settings [1]. However, the natural motion of the tibiofemoral joint is three-dimensional, activity-dependent, and varies across participants, determined by the complex interactions between the ligaments, articulating surfaces of the bones and the load transmitted by the knee [2,3]. Thus, quantifying how variations in tibiofemoral geometry affect calculations of musculoskeletal function is important to both researchers and clinicians interested in movement biomechanics.

During passive flexion-extension movements of the knee, tibiofemoral motion is three-dimensional and highly reproducible [3]. Smoger et al. (2015) showed that knee size and condylar geometry determine anterior–posterior tibiofemoral translation, while Ottoboni et al. (2010) used ligament and articular surface geometry to accurately model the three-dimensional tibiofemoral motion during passive knee flexion [5]. Normal walking and non-weight-bearing knee flexion exercises induce, respectively, 3.1 ± 2.4 mm and 2.6 ± 2.1 mm of anterior tibial translation [2]. Therefore, it appears that tibiofemoral motion during less strenuous activities like walking may be largely attributable to tibiofemoral geometry. Yet, the distinct effects of knee geometry and elasticity on musculoskeletal function is yet unclear.

Musculoskeletal modelling is finding increasing use in both clinical and research settings [1]. The range of applications is broad, ranging from studies of fetal development [6], femoral neck mechanics [7] , human motion [8] and knee mechanics [9], and focuses both on personalized [10] and cohort averages of different parameters of musculoskeletal function such as joint motion and muscle forces, either for selected tasks or multiple activities [7,11,12]. Such a variety of applications and objectives commonly requires a compromise between accuracy and complexity in each specific application.

Compliant tibiofemoral joint models provide an elastic, load-dependent, representation of tibiofemoral motion and typically require complex model generation and solution processes [9,10]. For example, Navacchia and co-workers (2019) used knee geometry extracted from both CT and MRI images and ligament material properties calibrated to in vitro laxity tests to iteratively solve the tibiofemoral elastic and motion problem in 76 – 210 minutes for two participants executing a single stride and chair rise cycle. In contrast, rigid tibiofemoral joint models provide a load-independent representation of tibiofemoral motion and are therefore exclusively based on geometry. Rigid modelling enables computationally efficient analyses for large cohorts, multiple activities and repeated tasks [8,11,13–15]. Most often, a generic musculoskeletal model is scaled to each participant using measurements of inter-segmental lengths [16]. On some occasions tibiofemoral motion is represented by simple revolute, planar and spherical joint models [8,14]. On other occasions, tibiofemoral motion is modelled by more complex articulated joint mechanisms explicitly imposing the consistency between tibiofemoral motion, articular surface and ligament geometry [17,18]. However, no study has compared the tibiofemoral motion in the model against corresponding measurements obtained during normal physical activity.

Here, we hypothesise that variation of tibiofemoral articular surface and ligament geometry determine variation of tibiofemoral motion and musculoskeletal function. To test this hypothesis, we aimed at 1) modelling the variation of tibiofemoral motion exclusively using variations of tibiofemoral geometry in healthy adults; and 2) studying the effect of geometrical variation of tibiofemoral motion on musculoskeletal function. The geometry-based tibiofemoral motion was modelled by prescribing the consistency between the tibiofemoral motion, the articular surface and the ligament geometry. The variation of the geometry-based tibiofemoral motion was obtained by embedding in the model variations of knee size in one cohort and validated against corresponding bi-planar fluoroscopy measurements of all the six motion components obtained in a second independent cohort [19]. The effect of tibiofemoral geometry on musculoskeletal function was studied by comparing matched musculoskeletal models embedding the geometry-based tibiofemoral motion and a common generic tibiofemoral joint model of reference. Geometry-based and scaled-generic joint angles, net moments, muscle and joint forces for six different normal activity types were calculated and compared.

2. Materials and Methods

2.1 Imaging and motion data

Computed-Tomography (CT) images and motion data for one cohort of 12 healthy participants (females, age: 67 ± 5 years, weight: 75 ± 14 kg, height: 159 ± 7 cm) were obtained from our earlier work [7,20]. In summary, CT images of the distal femur and the proximal tibia were obtained using a clinical whole-body scanner (Aquilon CT, Toshiba Corporation, Tokyo). Motion data were comprised of trajectories of 46 skin-mounted reflective markers and ground reaction forces. The motion data were recorded for a static pose, normal walking, fast walking, jumping, stair ascent, stair descent, rising from and sitting down onto a chair. Full details of the marker set were reported by Dorn et al. (2012) [21].

2.2 Dynamic bi-planar fluoroscopy measurements of tibiofemoral motion

Mobile bi-plane fluoroscopy measurements of tibiofemoral joint motion while walking (1.03 – 1.51 m/s) were obtained for a second independent cohort by Gray et al. (2019). The cohort comprised fifteen healthy individuals (age: 31 ± 6 years, weight: 67 ± 8 kg, height: 168 ± 9 cm) with no knee pain and history of knee surgery [19]. The study provided mean and standard deviation for all six motion components in the tibiofemoral coordinate system by Grood and Suntay (1983) [22].

2.3 Scaled-generic musculoskeletal modelling

Full-body scaled-generic musculoskeletal models were obtained earlier [7,14] by scaling the generic model described by Dorn et al. (2012)[21], an evolution of the generic model 'gait2392' provided with OpenSim embedding the planar tibiofemoral joint motion created by Yamaguchi and Zajac (1989)[23]. The generic model was fitted to each participant's mass and inter-segment distances using OpenSim's built-in scaling function [16]. The tibiofemoral motion was scaled to the participants using the distance between the anterior superior iliac spine and the lateral epicondyles (thigh length). The validity of the model was assessed by comparing joint and muscle forces in the model to corresponding published measurements [7,14].

2.4 Geometry-based musculoskeletal modelling

The variation of tibiofemoral geometry in the cohort was described by scaling a baseline anatomy to match width and depth of both the femoral and tibial bones because size differences largely explain the variation of tibiofemoral motion in healthy adults [4]. The baseline anatomy included the bone surfaces of the tibia and the femur, the cartilaginous articular surfaces and ligament insertions (Anterior Cruciate Ligament, ACL; Posterior Cruciate Ligament, PCL; Medial Collateral

Ligament, MCL) from a healthy male donor (height: 173 cm; mass: 61.2 kg). The proximal tibia and distal femur in the participants were segmented from the CT images (ScanIP, Simpleware, Exeter, UK). The width and depth of tibial and femoral condyles were measured from the segmented bone geometries. Antero-posterior and medio-lateral scaling factors were determined by scaling the baseline bone geometry to the width and depth of the tibia and the femur in the participants (Table S6). The articular surfaces of the cartilage, the ligaments origin and insertion in the baseline anatomy were then scaled to each participant. Anatomical reference systems were created for the tibia and femur using the skeletal surfaces [24] assuming the tibia longitudinal axis coincident with the longitudinal axis in the images because the distal tibia was not available (Figure 1).

The geometry-based tibiofemoral motion was calculated using a parallel mechanism. The procedure was described and validated earlier against experimental measurement for all six motion components by Conconi et al. (2018)[25]. The geometry-based tibiofemoral joint motion was determined by prescribing uniform ligament lengths and continuous contact of the articular surfaces over 120° of knee flexion [25]. Firstly, the tibiofemoral joint motion was estimated by minimizing a geometrical estimator of the peak contact pressure over intermediate knee flexion angles [26,27]. Next, a single-degree-of-freedom spatial parallel mechanism was generated composed of the femur and tibia connected by five struts. Three of the five struts were defined using the attachment sites of the ACL, PCL and MCL. The remaining two struts were defined using the curvature of the femoral and tibial condyles. Finally, the spatial linkage was synthetized by optimizing the coordinates of the ligaments' attachment points and the lengths of the five struts within a 2 mm variation to best match the initial estimate of tibiofemoral joint motion [24] (Figure 1).

The geometry-based tibiofemoral pose was calculated using the spatial linkage at 2° intervals between 0° and 120° knee flexion. Then, the tibiofemoral pose was decomposed into translations and Euler angles (i.e., tibiofemoral abduction, flexion and external rotation). The tibiofemoral pose in the CT images was assumed 0° of knee flexion. The geometry-based musculoskeletal model was obtained by duplicating the scaled-generic model and by implementing the geometry-based tibiofemoral motion using a custom joint in OpenSim. The parent (femur) coordinate system in the geometry-based tibiofemoral joint model was aligned to the parent coordinate system in the scaled-generic knee model. Tibiofemoral joint translations and rotations were expressed as a function of the knee flexion angle using cubic splines. The hip-to-knee and knee-to-ankle distances were matched to those in the scaled-generic model to ensure identical leg lengths in both models at zero knee flexion (Figure 1).

The geometry-based musculoskeletal function for normal walking, fast walking, jumping, stair ascent, stair descent, rising from and sitting down onto a chair was calculated using the same inverse kinematic and static optimization procedures used earlier for the scaled-generic models [7,20].

2.5 Data analysis

The six motion components while walking in geometry-based and scaled-generic models generated for the first cohort was compared to corresponding measurements in the second independent cohort of healthy adults (aim 1).

The effect of tibiofemoral geometry on musculoskeletal function (aim 2) was the difference between geometry-based and scaled-generic outputs. Muscle and joint reaction forces were normalized by participants' body weight (BW). Joint angles, net joint moments, muscle forces and joint reaction forces in different participants and activities were pooled and analysed using linear regression analysis. Average and peak differences were assessed using the Root Mean Square Error (RMSE) and the 98th percentile of the difference distribution. Percentage differences were calculated using the scaled-generic range of joint angles, peak net joint moments, peak muscle forces, and peak joint reaction forces across activities.

3. Results

Consistent with Gray et al. (2019), the geometry-based tibiofemoral joint while walking was slightly bent (1° – 12°) at heel-strike, reached its maximum flexion (9° – 23°) at contralateral toe-off (CTO) and then extended to a minimum flexion angle (0° – 9°) before rapidly flexing to 63° – 70° knee flexion at 70% gait cycle (Figure 2A). The knee abduction angle (-7 – -2°) and distraction (-4 – 0 mm) showed relatively small changes over the gait cycle. The range of knee external rotation was -8° – 7° during stance and reached the peak internal rotation at peak knee flexion during swing (0° – 13°). The knee lateral translation showed modest changes during stance (-1.5 – 3.5 mm) before translating medially during late stance and early swing (-3.2 – 2.0 mm). Also consistent with the reference measurements was the variation across participants of the tibial anterior translation (± 2.5 mm). However, the pattern of the tibial anterior translation did not capture the anterior shift observed between heel strike and contralateral toe-off (2.7 – 2.8 mm) and during early swing (5.3 mm). Also, the range of tibiofemoral flexion (63° on average) was smaller than that in the fluoroscopy measurements (68° on average).

The scaled-generic and geometry-based tibiofemoral flexion angle were practically identical (R^2 = 1) (Figure 2B) and both provided comparable patterns for the remaining 5 motion components, except for 8 mm anterior translation offset and increased scaled-generic anterior translation and distraction during swing. However, the variance in the scaled-generic tibiofemoral motion was smaller than that in the fluoroscopy measurements for tibia anterior translation and distraction (0.9 mm and 0.7 mm) and zero for tibiofemoral abduction, external rotation and lateral translation, as prescribed in the tibiofemoral model of reference.

The effect of variation of tibiofemoral geometry on musculoskeletal function was modest in cohort averages of all the musculoskeletal outputs (Figures 3 – 7). When all results were pooled, the range of the coefficient of determination between scaled-generic and geometry-based model outputs was 0.60 – 1 in overall (Figures 3 – 5). Average differences in hip, knee and ankle angles were less than 0.5 – 4.0° and peak difference reached 14° for the hip rotation (29.5%) (Figure 3). Average differences in net joint moments were 0.6 – 4.2 Nm while peak differences reached 20.4 Nm at the knee (32.7%) (Figure 4). Average differences in joint reaction forces were 0.37 – 0.47 BW and peak differences reached 1.3 – 2.1 BW (30 – 36%) (Figure 5). Average difference in muscle forces were 0 – 0.26 BW and the peak difference was 0.01 – 1.00 BW (Figure 6 – 7).

By pooling the results activity-by-activity, the peak difference between scaled-generic and geometry-based joint angles was less than 1° across activities and joints. Net joint moment varied by less than 1.7 Nm for all activities and joints, except for 6.3 Nm difference found at the ankle between normal walking and rising from and sitting on a chair. Joint reaction forces varied from 0.31 – 0.58 BW for walking to 1.77 – 2.94 BW for stair descent. Muscle forces varied from 0.01 – 0.36 BW for walking to 0 – 2.45 BW for jumping (Table S2 – S5, Supplementary Material).

4. DISCUSSION

We hypothesised that variation of tibiofemoral geometry determines variations in tibiofemoral motion and musculoskeletal function. We calculated a geometry-based tibiofemoral motion exclusively based on variation of tibiofemoral geometry in a cohort of healthy adults and compared the calculated motion to corresponding fluoroscopy measurements for all six planes of motion in a second independent cohort (aim 1). The effect of tibiofemoral geometry on musculoskeletal was studied by comparing matched musculoskeletal models embedding the geometry-based and a generic tibiofemoral motion. We found that 1) the tibiofemoral geometry variation is the major determinant of tibiofemoral motion during walking in healthy adults; and 2) the tibiofemoral geometry variation has moderate effect on cohort averages of musculoskeletal function and large effect on musculoskeletal function for individual instances of the cohort, particularly when muscle and joint forces are of interest.

Variation of tibiofemoral geometry is a major determinant of tibiofemoral motion in healthy adults during normal activity because the tibiofemoral motion determined exclusively using geometrical information of the tibiofemoral joint described most of the variation in corresponding fluoroscopy measurements during walking. The major differences included the smaller range of knee flexion attributable to the age difference between the present cohort (age: 67 ± 5) and the younger cohort (31 ± 6 years) that provided the fluoroscopy measurements [28]. Also, the geometry-based tibiofemoral motion did not capture the anterior tibial shift during early stance (2.7 –

2.8 mm) and early swing (5.3 mm; 60 – 80% gait) in the fluoroscopy measurements (Figure 2A), which may be partially attributed to the knee compliance not included in the model. Nevertheless, the geometry-based tibiofemoral motion displayed similar variation to corresponding fluoroscopy measurements for all the six motion components and similar pattern for five motion components, hence supporting our hypothesis that tibiofemoral geometry determines tibiofemoral motion during normal activity. This finding is in line with the association between articular surface geometry and tibiofemoral motion during squatting exercises reported by Smoger et al. (2015) [4] and it expands its validity to the geometry of the ligaments, and to walking.

The scaled-generic tibiofemoral motion provided a valid reference for studying the effect of tibiofemoral geometry on musculoskeletal function. In fact, the scaled-generic tibiofemoral motion showed consistent pattern but smaller variance in all the secondary planes of motion as compared to corresponding fluoroscopy measurements. We found that variation of tibiofemoral geometry affects moderately cohort averages of musculoskeletal function across all the musculoskeletal outputs analysed (R^2 = 0.60 – 1). The size of the cohort used in this study (n=12) appears adequate for studying cohort averages of every musculoskeletal model output including muscle forces, which were most sensitive to changes in tibiofemoral motion (Figure 6 and Figure S1). Scaled-generic models are therefore valid and efficient solutions for determining, for example, the main effect of a clinical intervention [29]. Nevertheless, variation of tibiofemoral geometry had a non-negligible effect in individual instances of the model causing variation of musculoskeletal function reaching 1 – 2.45 BW for muscle and joint forces. This finding is consistent with the notion that consistency between tibiofemoral geometry and motion is important in the context of personalized applications (within participant), particularly for studying muscle and joint forces [9].

The consistency between the geometry-based tibiofemoral joint motion calculated here and corresponding measurements obtained in vivo [19] is in line with earlier validation studies showing that the parallel mechanism used here can provide an accurate representation of tibiofemoral motion in a single participant [30] and four knee specimens [5,24]. The present study demonstrates the robustness of the method for a cohort of healthy participants for which only the skeletal geometry is available for studying cohort-based variation of tibiofemoral motion. Yet, the validity of the present modelling procedure for studying personalized musculoskeletal function remains unclear because no bi-planar fluoroscopy measurements of tibiofemoral motion were available for the present cohort. The effect of geometrical variations of the tibiofemoral joint on the hip joint force reported here is similar to that caused by anatomical errors committed while scaling a generic musculoskeletal model to a specific participant (0.2 – 0.7 BW) [20,31] and smaller than that caused by skin-motion artefacts (1.5 – 1.8 BW) [32] and potentially caused by muscle co-contraction (8 – 10 BW) [13]. Therefore, it appears that studying personalized features of musculoskeletal function requires accurate information of every anatomical and functional parameter in the model, including tibiofemoral joint motion.

One limitation of the present study is the rigid tibiofemoral motion assumption that prevents studying tibiofemoral motion changes in functional tasks of variable demand. Nevertheless, our aim was to examine the independent effect of tibiofemoral geometry. The present results are relevant to a broad range of applications of rigid-body modelling [8,11,13–15]. The spatial linkage described here can be extended to account for the elasticity of each ligament [33] or their lumped effect into a single knee compliance matrix [34], hence potentially providing an alternative solution to current methods for modelling the knee joint compliance [9,10]. Finally, the effect of tibiofemoral geometry on musculoskeletal function reported here was determined using as reference a common generic tibiofemoral model [23] scaled to the cohort using marker-based measurements of thigh length. Other generic tibiofemoral models [35] and methods for fitting a generic musculoskeletal model to the participant [36] may provide a valid alternative to the scaled-generic model used here. However, the scaled-generic model used here provided a common and valid motion of reference for isolating the effect of tibiofemoral geometry on musculoskeletal function.

In conclusion, tibiofemoral motion during walking is mostly determined by tibiofemoral geometry. Variation of tibiofemoral motion on musculoskeletal function is on average modest, supporting the use of a generic tibiofemoral joint models for studying the main effect of intervention in large cross-sectional studies. Nevertheless, musculoskeletal function in specific individuals often requires information of tibiofemoral geometry, particularly when estimates of muscle and joint forces are of interest. The present findings expand knowledge of movement biomechanics and can inform the decision-making process for modelling musculoskeletal function.

ACKNOWLEDGMENTS

The Australian Research Council (DP180103146; FT180100338) and the State Government of South Australia are gratefully acknowledged. The authors would also thank Mr. Mark Williams for his contribution to coding.

REFERENCES

[1] J.L. Hicks, T.K. Uchida, A. Seth, A. Rajagopal, S.L. Delp, Is my model good enough? Best practices for verification and validation of musculoskeletal models and simulations of movement., J. Biomech. Eng. 137 (2015) 020905. doi:10.1115/1.4029304.

[2] C. a. Myers, M.R. Torry, K.B. Shelburne, J.E. Giphart, R.F. LaPrade, S.L.-Y. Woo, J.R. Steadman, In Vivo Tibiofemoral Kinematics During 4 Functional Tasks of Increasing Demand Using Biplane Fluoroscopy, Am. J. Sports Med. 40 (2012) 170–178. doi:10.1177/0363546511423746.

[3] L. Blankevoort, R. Huiskes, A. De Lange, Helical axes of passive knee joint motions, J. Biomech. 23 (1990) 1219–1229. doi:10.1016/0021-9290(90)90379-H.

[4] L.M. Smoger, C.K. Fitzpatrick, C.W. Clary, A.J. Cyr, L.P. Maletsky, P.J. Rullkoetter, P.J. Laz, Statistical modeling to characterize relationships between knee anatomy and kinematics, J. Orthop. Res. 33 (2015) 1620–1630. doi:10.1002/jor.22948.

[5] A. Ottoboni, V. Parenti-Castelli, N. Sancisi, C. Belvedere, A. Leardini, Articular surface approximation in equivalent spatial parallel mechanism models of the human knee joint: An experiment-based assessment, Proc. Inst. Mech. Eng. Part H J. Eng. Med. 224 (2010) 1121–1132. doi:10.1243/09544119JEIM684.

[6] S.W. Verbruggen, B. Kainz, S.C. Shelmerdine, O.J. Arthurs, J. V. Hajnal, M.A. Rutherford, A.T.M. Phillips, N.C. Nowlan, European Society of Biomechanics S.M. Perren Award 2018: Altered biomechanical stimulation of the developing hip joint in presence of hip dysplasia risk factors, J. Biomech. 78 (2018) 1–9. doi:10.1016/J.JBIOMECH.2018.07.016.

[7] M.E. Kersh, S. Martelli, R.M.D. Zebaze, E. Seeman, M.G. Pandy, Mechanical Loading of the Femoral Neck in Human Locomotion., J. Bone Miner. Res. 33 (2018) 1999–2006. doi:10.1002/jbmr.3529.

[8] R. Dumas, F. Moissenet, X. Gasparutto, L. Cheze, Influence of joint models on lower-limb musculo-tendon forces and three- dimensional joint reaction forces during gait, Spec. Issue Artic. Proc IMechE Part H J Eng. Med. 226 (2012) 146–160. doi:10.1177/0954411911431396.

[9] P. Gerus, M. Sartori, T.F. Besier, B.J. Fregly, S.L. Delp, S.A. Banks, M.G. Pandy, D.D. D'Lima, D.G. Lloyd, Subject-specific knee joint geometry improves predictions of medial tibiofemoral contact forces., J. Biomech. 46 (2013) 2778–86. doi:10.1016/j.jbiomech.2013.09.005.

[10] A. Navacchia, D.R. Hume, P.J. Rullkoetter, K.B. Shelburne, A computationally efficient strategy to estimate muscle forces in a finite element musculoskeletal model of the lower limb, J. Biomech. 84 (2019) 94–102. doi:10.1016/J.JBIOMECH.2018.12.020.

[11] H. Ziaeipoor, M. Taylor, M. Pandy, S. Martelli, A novel training-free method for real-time prediction of femoral strain, J. Biomech. 86 (2019) 110–116. doi:10.1016/J.JBIOMECH.2019.01.057.

[12] H. Ziaeipoor, S. Martelli, M.G. Pandy, M. Taylor, Efficacy and efficiency of multivariate linear regression for the rapid prediction of the femoral strain field during activity, Med. Eng. Phys. 63 (2019) 88–92. doi:10.1016/j.medengphy.2018.12.001.

[13] S. Martelli, D. Calvetti, E. Somersalo, M. Viceconti, Stochastic modelling of

muscle recruitment during activity, Interface Focus. 5 (2015) 20140094-. doi:10.1098/rsfs.2014.0094.

[14] S. Martelli, G. Valente, M. Viceconti, F. Taddei, Sensitivity of a subject-specific musculoskeletal model to the uncertainties on the joint axes location., Comput. Methods Biomech. Biomed. Engin. 18 (2015) 1555–63. doi:10.1080/10255842.2014.930134.

[15] E.M. Arnold, S.R. Ward, R.L. Lieber, S.L. Delp, A model of the lower limb for analysis of human movement., Ann. Biomed. Eng. 38 (2010) 269–79. doi:10.1007/s10439-009-9852-5.

[16] S.L. Delp, F.C. Anderson, A.S. Arnold, P. Loan, A. Habib, C.T. John, E. Guendelman, D.G. Thelen, OpenSim: open-source software to create and analyze dynamic simulations of movement, IEEE Trans. Biomed. Eng. 54 (2007) 1940–1950. doi:10.1109/TBME.2007.901024.

[17] M. Barzan, L. Modenese, C.P. Carty, S. Maine, C.A. Stockton, N. Sancisi, A. Lewis, J. Grant, D.G. Lloyd, S. Brito da Luz, Development and validation of subject-specific pediatric multibody knee kinematic models with ligamentous constraints, J. Biomech. 93 (2019) 194–203. doi:10.1016/j.jbiomech.2019.07.001.

[18] S. Brito da Luz, L. Modenese, N. Sancisi, P.M. Mills, B. Kennedy, B.R. Beck, D.G. Lloyd, Feasibility of using MRIs to create subject-specific parallel-mechanism joint models, J. Biomech. 53 (2017) 45–55. doi:10.1016/j.jbiomech.2016.12.018.

[19] H.A. Gray, S. Guan, L.T. Thomeer, A.G. Schache, R. de Steiger, M.G. Pandy, Three-dimensional motion of the knee-joint complex during normal walking revealed by mobile biplane x-ray imaging, J. Orthop. Res. 37 (2019) 615–630. doi:10.1002/jor.24226.

[20] S. Martelli, M.E. Kersh, M.G. Pandy, Sensitivity of femoral strain calculations to anatomical scaling errors in musculoskeletal models of movement, J. Biomech. 48 (2015) 3615–24. doi:10.1016/j.jbiomech.2015.08.001.

[21] T.W. Dorn, A.G. Schache, M.G. Pandy, Muscular strategy shift in human running: dependence of running speed on hip and ankle muscle performance., J. Exp. Biol. 215 (2012) 1944–56. doi:10.1242/jeb.064527.

[22] E.S. Grood, W.J. Suntay, A joint coordinate system for the clinical description of three-dimensional motions: application to the knee, J. Biomech. Eng. 105 (1983) 136–144.

[23] G.T. Yamaguchi, F.E. Zajac, A planar model of the knee joint to characterize the knee extensor mechanism, J Biomech. 22 (1989) 1–10.

[24] N. Sancisi, V. Parenti-Castelli, A novel 3D parallel mechanism for the passive motion simulation of the patella-femur-tibia complex, Meccanica. 46 (2011) 207–220. doi:10.1007/s11012-010-9405-x.

[25] M. Conconi, N. Sancisi, V. Parenti-Castelli, Subject-Specific Model of Knee Natural Motion: A Non-invasive Approach, in: Proc. Adv. Robot., Springer, Cham, 2018: pp. 255–264. doi:10.1007/978-3-319-56802-7_27.

[26] M. Conconi, A. Leardini, V. Parenti-Castelli, Joint kinematics from functional adaptation: A validation on the tibio-talar articulation, J. Biomech. 48 (2015) 2960–2967. doi:10.1016/j.jbiomech.2015.07.042.

[27] M. Conconi, V. Parenti-Castelli, A sound and efficient measure of joint congruence, Proc. Inst. Mech. Eng. Part H J. Eng. Med. 228 (2014) 935–941. doi:10.1177/0954411914550848.

[28] J. Favre, J.C. Erhart-Hledik, T.P. Andriacchi, Age-related differences in

sagittal-plane knee function at heel-strike of walking are increased in osteoarthritic patients, Osteoarthr. Cartil. 22 (2014) 464–471. doi:10.1016/J.JOCA.2013.12.014.

[29] N.S. Thompson, R.J. Baker, A.P. Cosgrove, I.S. Corry, H.K. Graham, Musculoskeletal modelling in determining the effect of botulinum toxin on the hamstrings of patients with crouch gait., Dev. Med. Child Neurol. 40 (1998) 622–5. doi:10.1111/j.1469-8749.1998.tb15428.x.

[30] F. Nardini, N. Sancisi, C. Belvedere, M. Conconi, A. Leardini, V.P. Castelli, Definition of a subject-specific model of the knee in vivo, Gait Posture. 49 (2016) S6. doi:10.1016/j.gaitpost.2016.07.030.

[31] G. Lenaerts, W. Bartels, F. Gelaude, M. Mulier, A. Spaepen, G. Van der Perre, I. Jonkers, Subject-specific hip geometry and hip joint centre location affects calculated contact forces at the hip during gait, J. Biomech. 42 (2009) 1246–1251.

[32] G. Lamberto, S. Martelli, A. Cappozzo, C. Mazzà, To what extent is joint and muscle mechanics predicted by musculoskeletal models sensitive to soft tissue artefacts?, J. Biomech. 62 (2016) 68–76. doi:10.1016/j.jbiomech.2016.07.042.

[33] N. Sancisi, V. Parenti-Castelli, A sequentially-defined stiffness model of the knee, Mech. Mach. Theory. 46 (2011) 1920–1928. doi:10.1016/j.mechmachtheory.2011.07.006.

[34] G. Lamberto, D.B. Amin, L.B. Solomon, B. Ding, K.J. Reynolds, C. Mazzà, S. Martelli, Personalised 3D knee compliance from clinically viable knee laxity measurements: A proof of concept ex vivo experiment, Med. Eng. Phys. 64 (2018) 80–85. doi:10.1016/J.MEDENGPHY.2018.12.003.

[35] P.S. Walker, J.S. Rovick, D.D. Robertson, The effects of knee brace hinge design and placement on joint mechanics, J. Biomech. 21 (1988). doi:10.1016/0021-9290(88)90135-2.

[36] J. Zhang, H. Sorby, J. Clement, C.D.L. Thomas, P. Hunter, P. Nielsen, D. Lloyd, M. Taylor, T. Besier, The MAP Client: User-Friendly Musculoskeletal Modelling Workflows, in: Springer International Publishing, 2014: pp. 182–192. doi:10.1007/978-3-319-12057-7_21.

FIGURES

Figure 1 –The process involved segmentation of the CT images (A), bi-axial scaling (transversal plane) of the template geometry (B), calculation of the geometry-based tibiofemoral motion by imposing the consistency between the motion and the geometry of the ACL, PCL, MCL and spherical approximations (shaded spheres) of femoral and tibial condyles (C) and, substitution of the scaled-generic tibiofemoral motion in the scaled-generic model using the geometry-based tibiofemoral motion (D). The distance between the Right Anterior Superior Spine (RASIS) and the Lateral Epicondyle (LE) displayed in the figure were used to scale the generic musculoskeletal model to each participant.

Figure 2 – In figure 2A, the geometry-based tibiofemoral motion (shaded grey) compared to corresponding bi-planar fluoroscopy measurements (shaded red) for walking (mean ± 1SD). The average standing position (solid black and red lines), the heel-strike (HS), contralateral toe-off (CTO), contralateral heel-strike (CHS) and toe-off (TO) events are also displayed. In figure 2B, the geometry-based (shaded grey) and scaled-generic (shaded green) tibiofemoral motion (mean ± 1SD) compared to the mean fluoroscopy measurement (solid blue) in the OpenSim's knee coordinate system. The two separate comparisons (Figure 2A and 2B) were necessary because bi-planar fluoroscopy measurements for each individual participant were not available.

Figure 3 – Linear correlation analysis of scaled-generic and geometry-based joint angles.

Figure 4 – Linear correlation analysis of scaled-generic and geometry-based joint moments.

Figure 5 – Linear correlation analysis of scaled-generic and geometry-based joint forces.

Figure 6 – Scaled-generic (red) and geometry-based (grey) muscle force time histories during walking. The average muscle force pattern (solid line) and the one standard deviation band (shaded region) are displayed.

Figure 1

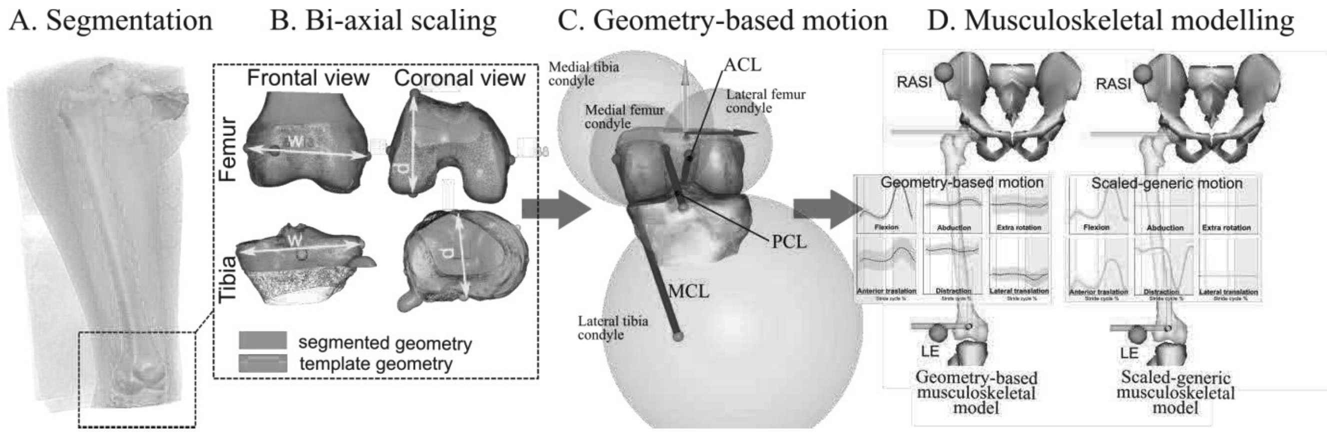
A. Segmentation
B. Bi-axial scaling
C. Geometry-based motion
D. Musculoskeletal modelling
Frontal view
Coronal view
Femur
Tibia
w
d
segmented geometry
template geometry
Medial tibia condyle
Medial femur condyle
ACL
Lateral femur condyle
PCL
MCL
Lateral tibia condyle
RASI
Geometry-based motion
Scaled-generic motion
Flexion
Abduction
Extra rotation
Anterior translation
Distraction
Lateral translation
LE
Geometry-based musculoskeletal model
Scaled-generic musculoskeletal model

Figure 2

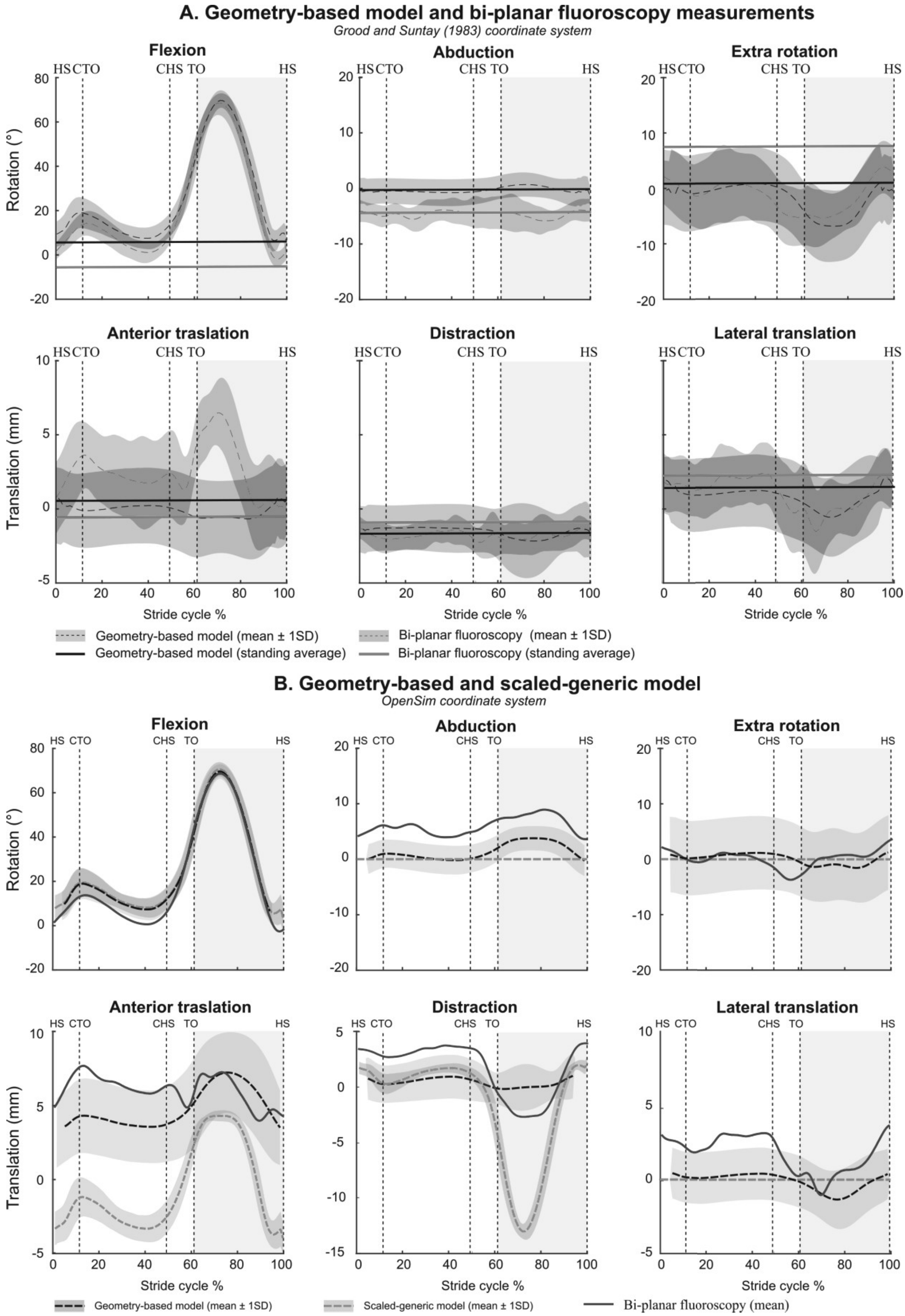

A. Geometry-based model and bi-planar fluoroscopy measurements
Grood and Suntay (1983) coordinate system
Flexion
Abduction
Extra rotation
Anterior traslation
Distraction
Lateral translation
HS CTO CHS TO HS
Rotation (°)
Translation (mm)
Stride cycle %
Geometry-based model (mean ± 1SD)
Geometry-based model (standing average)
Bi-planar fluoroscopy (mean ± 1SD)
Bi-planar fluoroscopy (standing average)
B. Geometry-based and scaled-generic model
OpenSim coordinate system
Flexion
Abduction
Extra rotation
Anterior traslation
Distraction
Lateral translation
Rotation (°)
Translation (mm)
Stride cycle %
Geometry-based model (mean ± 1SD)
Scaled-generic model (mean ± 1SD)
Bi-planar fluoroscopy (mean)

Figure 3

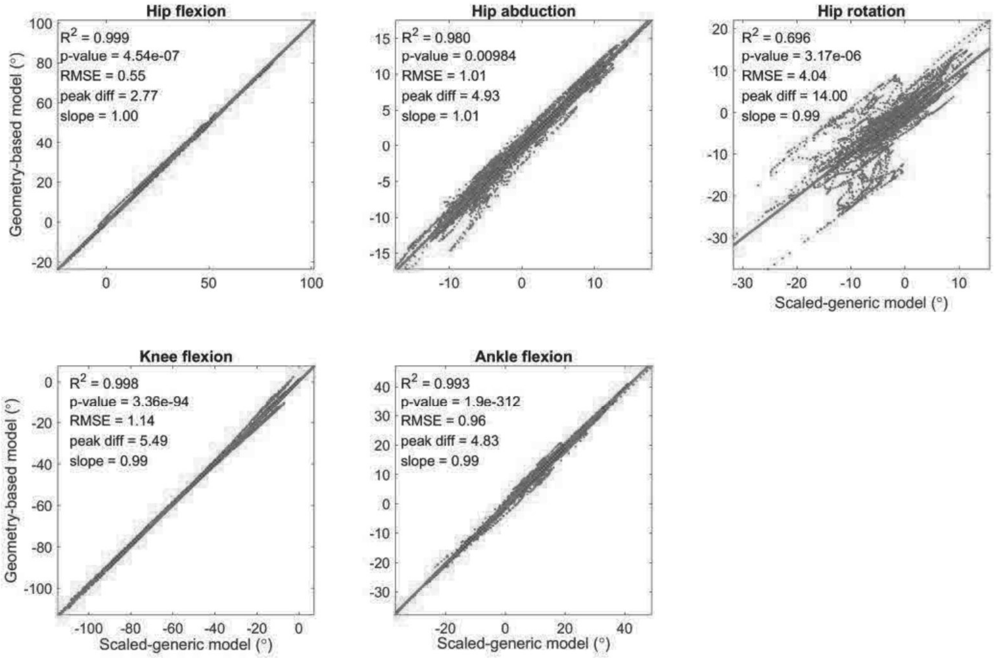
Hip flexion
R^2 = 0.999
p-value = 4.54e-07
RMSE = 0.55
peak diff = 2.77
slope = 1.00
Hip abduction
R^2 = 0.980
p-value = 0.00984
RMSE = 1.01
peak diff = 4.93
slope = 1.01
Hip rotation
R^2 = 0.696
p-value = 3.17e-06
RMSE = 4.04
peak diff = 14.00
slope = 0.99
Knee flexion
R^2 = 0.998
p-value = 3.36e-94
RMSE = 1.14
peak diff = 5.49
slope = 0.99
Ankle flexion
R^2 = 0.993
p-value = 1.9e-312
RMSE = 0.96
peak diff = 4.83
slope = 0.99
Geometry-based model (°)
Scaled-generic model (°)

Figure 4

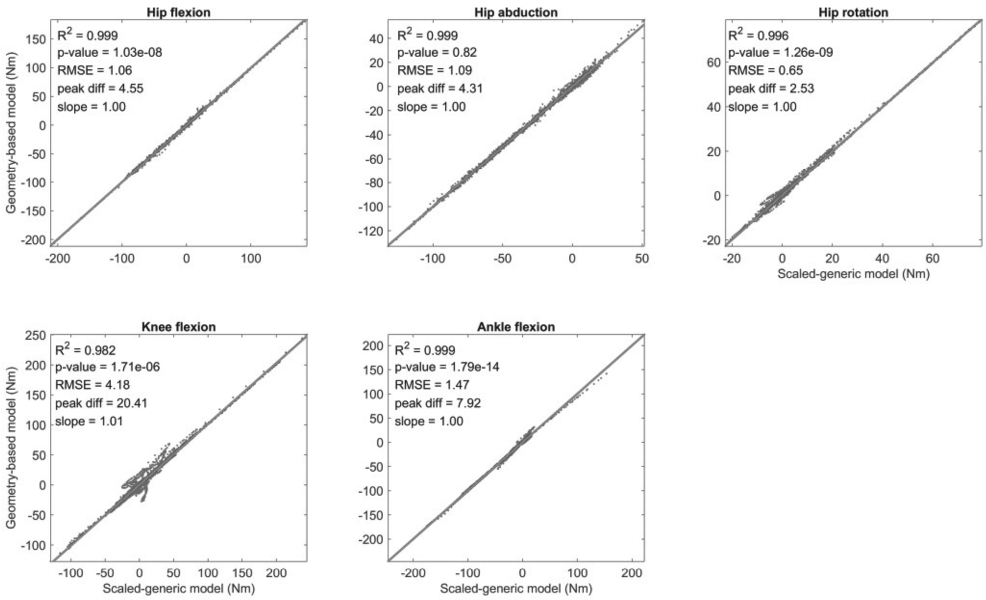
Hip flexion
R^2 = 0.999
p-value = 1.03e-08
RMSE = 1.06
peak diff = 4.55
slope = 1.00
Hip abduction
R^2 = 0.999
p-value = 0.82
RMSE = 1.09
peak diff = 4.31
slope = 1.00
Hip rotation
R^2 = 0.996
p-value = 1.26e-09
RMSE = 0.65
peak diff = 2.53
slope = 1.00
Knee flexion
R^2 = 0.982
p-value = 1.71e-06
RMSE = 4.18
peak diff = 20.41
slope = 1.01
Ankle flexion
R^2 = 0.999
p-value = 1.79e-14
RMSE = 1.47
peak diff = 7.92
slope = 1.00
Geometry-based model (Nm)
Scaled-generic model (Nm)

Figure 5

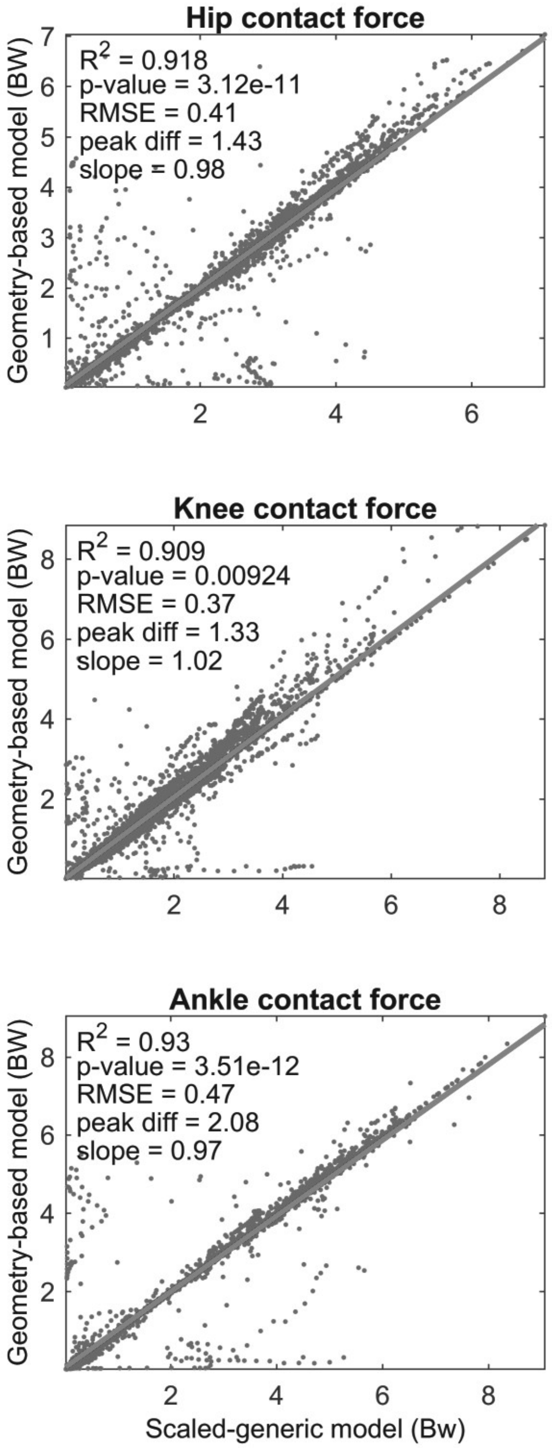
Hip contact force
R^2 = 0.918
p-value = 3.12e-11
RMSE = 0.41
peak diff = 1.43
slope = 0.98
Knee contact force
R^2 = 0.909
p-value = 0.00924
RMSE = 0.37
peak diff = 1.33
slope = 1.02
Ankle contact force
R^2 = 0.93
p-value = 3.51e-12
RMSE = 0.47
peak diff = 2.08
slope = 0.97
Geometry-based model (BW)
Scaled-generic model (Bw)

Figure 6

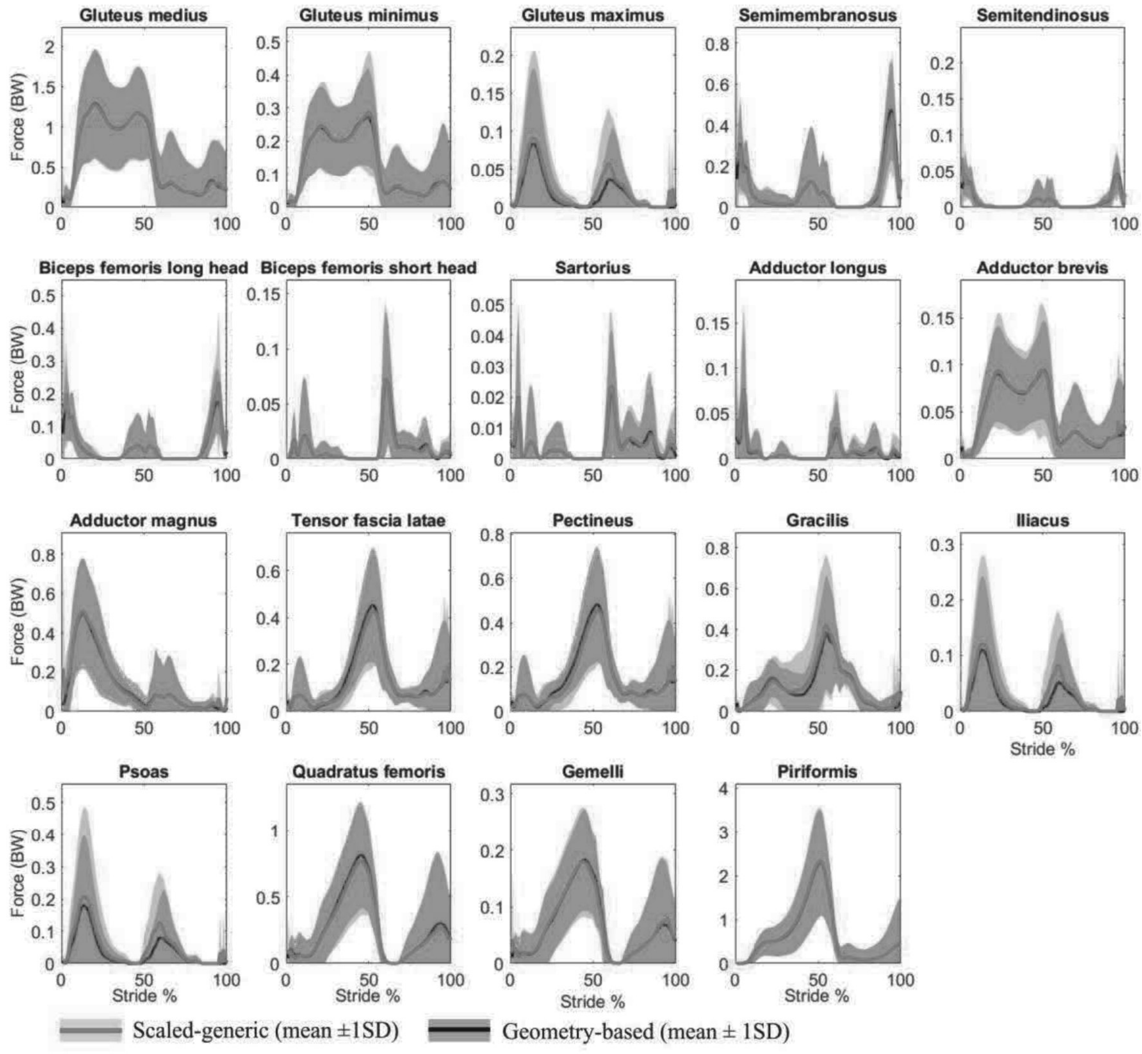
Gluteus medius
Gluteus minimus
Gluteus maximus
Semimembranosus
Semitendinosus
Biceps femoris long head
Biceps femoris short head
Sartorius
Adductor longus
Adductor brevis
Adductor magnus
Tensor fascia latae
Pectineus
Gracilis
Iliacus
Psoas
Quadratus femoris
Gemelli
Piriformis
Force (BW)
Stride %
Scaled-generic (mean ±1SD)
Geometry-based (mean ± 1SD)